Baku State University: Journal of Physics & Space Sciences, **2026**, v3 (2), pp. 85-95

journal homepage: http://bsuj.bsu.edu.az/en

Dielectric Properties of PVA+$GeBi_2Te_4$-Based Nanocomposites

Khatira Z. Mehtiyeva*, Imamaddin R. Amiraslanov,
Vidadi A. Bagiyev, Ziya S. Aliev

Advanced Materials Science R&D Center, Baku State University, Baku, Azerbaijan
R e c e i v e d 27-Apr.-2026; A c c e p t e d 10-Jun-2026
DOI: https://doi.org/10.30546/209501.101.2026.3.02.651

Abstract

$GeBi_2Te_4$/PVA nanocomposites were prepared by incorporating $GeBi_2Te_4$ nanopowders obtained by high-energy ball milling into a poly(vinyl alcohol) (PVA) matrix using the solution-casting method. The structural and morphological properties of the materials were investigated by X-ray diffraction (XRD) and scanning electron microscopy (SEM). The dielectric properties of the composites were studied by dielectric spectroscopy in the frequency range from 120 Hz to 10^6 Hz and at temperatures between 20 and 100 °C. The frequency and temperature dependences of the dielectric permittivity, dielectric loss function, dielectric loss tangent, and electrical conductivity were analyzed. The results revealed pronounced dielectric dispersion and relaxation behavior associated with Maxwell–Wagner–Sillars interfacial polarization at the $GeBi_2Te_4$/PVA interfaces. The electrical conductivity increased with increasing frequency and temperature, while the absence of percolation indicated that charge transport remained dominated by the polymer matrix. The obtained results demonstrate the potential of $GeBi_2Te_4$/PVA composites as functional dielectric materials.

Keywords: $GeBi_2Te_4$, poly(vinyl alcohol), nanocomposites, dielectric spectroscopy, Maxwell–Wagner–Sillars polarization, electrical conductivity.
PACS: 77.22.Gm; 72.80.Le

1. Introduction

Layered chalcogenide compounds have attracted considerable interest due to their structural characteristics and wide range of physical properties [1–5]. The presence of

*Corresponding author – Tel.: (+994) 51 444 05 11
e-mail address: xatira.mehtiyeva@bsu.edu.az; *ORCID ID*: 0009-0004-5346-093X

strong intralayer bonding and weak interlayer van der Waals interactions facilitates crystal cleavage, resulting in the formation of thin platelet-like structures [1–6]. The high surface-area-to-volume ratio of such particles contributes to an increased interfacial contact area when they are incorporated into a polymer matrix [5–8].

Particular attention has been paid to the preparation of micro- and nanosized forms of layered compounds. A reduction in particle size is accompanied by an increase in specific surface area and the fraction of interfacial regions, leading to enhanced surface effects and a greater contribution of processes occurring at phase boundaries [6–9]. As a result, the influence of the filler on the electrical, dielectric, and relaxation properties of the composite system increases significantly [9, 11].

It is well established that the properties of composite materials are determined not only by the nature of their constituents but also by the size, concentration, and morphology of the filler particles [7–10]. The incorporation of micro- and nanostructured particles into a polymer matrix makes it possible to tailor charge transport mechanisms, space-charge accumulation, and polarization processes. Therefore, the use of layered semiconducting materials as fillers is of considerable interest for the development of new functional composites with tunable electrophysical properties [9–11].

One of the promising representatives of layered chalcogenides is $GeBi_2Te_4$ [12–14]. $GeBi_2Te_4$ belongs to the family of tetradymite-like tellurides and possesses a rhombohedral layered crystal structure [12–14]. Owing to its structural features and electronic properties, this material has attracted attention as a subject of research in the fields of thermoelectric and topological materials [12–14]. Furthermore, the ability of $GeBi_2Te_4$ to form platelet-like particles with a well-developed surface makes it a promising filler for polymer composites [12–14].

In recent years, considerable attention has been devoted to polymer composites containing layered and semiconducting fillers, since their incorporation enables effective tuning of the dielectric characteristics of the material [9–11].

In the present work, poly(vinyl alcohol) (PVA) was used as the matrix material because of its excellent film-forming ability, chemical stability, and capacity to ensure a uniform distribution of dispersed filler throughout the material volume [15, 16]. The use of PVA as a dielectric matrix makes it possible to investigate the influence of $GeBi_2Te_4$ particles on polarization processes and charge transport in the composite system [15, 16].

It should be noted that the influence of telluride-based fillers on the dielectric properties of polymer matrices has been studied only to a limited extent. For example, in LDPE+Bi_2Te_3 composites, the incorporation of telluride filler was found to cause significant changes in dielectric permittivity and dielectric loss due to interfacial polarization and charge transport processes [17]. However, information regarding the dielectric properties of $GeBi_2Te_4$/PVA composites is virtually absent from the literature.

To investigate these processes, dielectric spectroscopy was employed, as it provides information on polarization mechanisms, relaxation phenomena, and the electrical response of materials over a wide frequency range [15, 18].

The aim of the present work is to investigate the dielectric properties of $GeBi_2Te_4$/PVA composites and to determine the influence of $GeBi_2Te_4$ particles on polarization processes and dielectric losses in the polymer matrix.

2. Experimental Section

2.1. Preparation of $GeBi_2Te_4$ Nanopowder

$GeBi_2Te_4$ nanopowder was prepared by high-energy ball milling using the top-down approach [19, 20]. This method enables particle size reduction while preserving the chemical composition and crystal structure of the bulk starting material.

Single crystals of $GeBi_2Te_4$ synthesized from high-purity elements in evacuated quartz ampoules by the directional crystallization method were used as the starting material. The obtained ingots were first ground in an agate mortar to produce a homogeneous powder.

Further milling was carried out using a FRITSCH Pulverisette 6 planetary ball mill equipped with an 80 mL grinding vial and hardened stainless-steel (Fe–Cr) balls. Approximately 1 g of powder was milled at a ball-to-powder weight ratio of 10:1 and a rotation speed of 650 rpm for up to 40 h.

The layered structure of $GeBi_2Te_4$, characterized by weak van der Waals interactions between structural blocks, facilitates efficient particle fragmentation during mechanical treatment. As a result, powders with particle sizes in the nanometer range were obtained, as confirmed by X-ray diffraction and scanning electron microscopy analyses.

2.2. Preparation of the $GeBi_2Te_4$/PVA Composite

The $GeBi_2Te_4$/PVA composite was prepared by the solution-casting method. To prepare the polymer matrix, 0.2 g of poly(vinyl alcohol) (PVA) was dissolved in 10 mL of distilled water under continuous magnetic stirring until a clear and homogeneous solution was obtained.

After complete dissolution of the polymer, 0.2 g of $GeBi_2Te_4$ nanopowder was added to the solution. The resulting suspension was subjected to ultrasonic treatment to ensure a uniform distribution of filler particles throughout the polymer matrix.

The mixture was then kept at room temperature until the solvent had completely evaporated and the $GeBi_2Te_4$/PVA composite material had formed.

2.3. Characterization Methods

2.3.1. X-ray Diffraction Analysis

Phase analysis was performed using a Bruker D8 Endeavor X-ray diffractometer equipped with Cu Kα radiation (λ = 1.5406 Å). The diffraction patterns were collected in the θ–2θ geometry at an operating voltage of 40 kV and a tube current of 40 mA. The obtained diffraction patterns were used to identify the phase composition of the samples and to verify the preservation of the $GeBi_2Te_4$ crystal structure during the milling process.

2.3.2. Scanning Electron Microscopy and Energy-Dispersive X-ray Analysis

The morphology and microstructure of the samples were investigated by scanning electron microscopy using a field-emission scanning electron microscope (FE-SEM JSM-5600LV, JEOL, Japan). The micrographs were used to evaluate the shape and size of the particles after high-energy ball milling.

2.3.3. Dielectric Measurements

The dielectric properties of the $GeBi_2Te_4$/PVA composite were investigated using an E7-20 impedance analyzer. Measurements were performed over a wide frequency range at temperatures from 20 to 100°C.

The sample was placed in a measuring cell with parallel-plate electrodes to ensure stable electrical contact throughout the measurements. Temperature-dependent measurements were recorded under controlled heating conditions.

Based on the experimentally measured impedance values, the complex dielectric permittivity, dielectric loss tangent, and electrical conductivity were calculated. The obtained data were analyzed as functions of frequency and temperature.

3. Results and Discussion

3.1. Phase Identification and Morphological Characterization of PVA-$\boldsymbol{GeBi_2Te_4}$

3.1.1. Phase Identification by PXRD

The PXRD pattern of the PVA–$GeBi_2Te_4$ composite is presented in Figure 1. The diffraction profile exhibits a combination of broad and weak features together with several distinguishable peaks, reflecting the composite nature of the material.

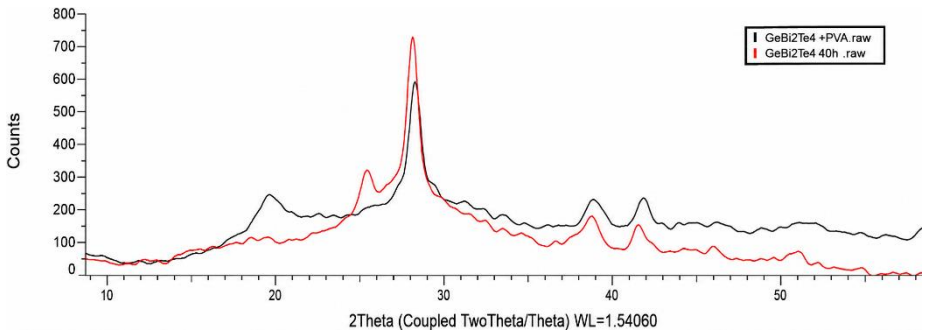

Figure 1. PXRD pattern of the PVA– $\boldsymbol{GeBi_2Te_4}$ composite showing the coexistence of amorphous PVA and crystalline $\boldsymbol{GeBi_2Te_4}$ phases.

The broad background and diffuse halo observed over a wide 2θ range are characteristic of the amorphous PVA matrix, indicating that the polymer phase dominates the overall diffraction pattern. In contrast, the presence of distinct diffraction peaks, particularly in the region around ~28° and 38–43° (2θ), can be attributed to the crystalline $GeBi_2Te_4$ phase embedded within the polymer matrix.

Compared to the PXRD pattern of the milled $GeBi_2Te_4$ powder, the peaks in the composite are significantly reduced in intensity and broadened, which can be explained by the combined effects of nanoscale particle size, reduced crystallinity, and the dilution of the crystalline phase within the amorphous polymer. The absence of additional sharp peaks indicates that no new crystalline phases were formed during the composite preparation process.

Overall, the PXRD results confirm that $GeBi_2Te_4$ nanoparticles are successfully incorporated into the PVA matrix while retaining their crystalline nature, although with reduced structural ordering due to nanoscale dispersion and interaction with the polymer phase.

3.1.2. SEM-EDX characterization

The morphology of the milled $GeBi_2Te_4$ powders was investigated by SEM, as shown in Figure 2. The image reveals the formation of irregularly shaped, agglomerated particles with sizes predominantly in the nanometer range.

The observed particle sizes vary approximately from ~60 nm to ~100 nm, indicating effective size reduction during the high-energy ball milling process. The particles tend to form agglomerates, a characteristic of nanoscale materials due to their high surface energy.

The morphology suggests that the layered structure of $GeBi_2Te_4$ facilitates fragmentation into fine particles during milling. The obtained nanostructured powder provides a large surface area and increased number of interfaces, which can significantly influence the electrical properties of the composite material.

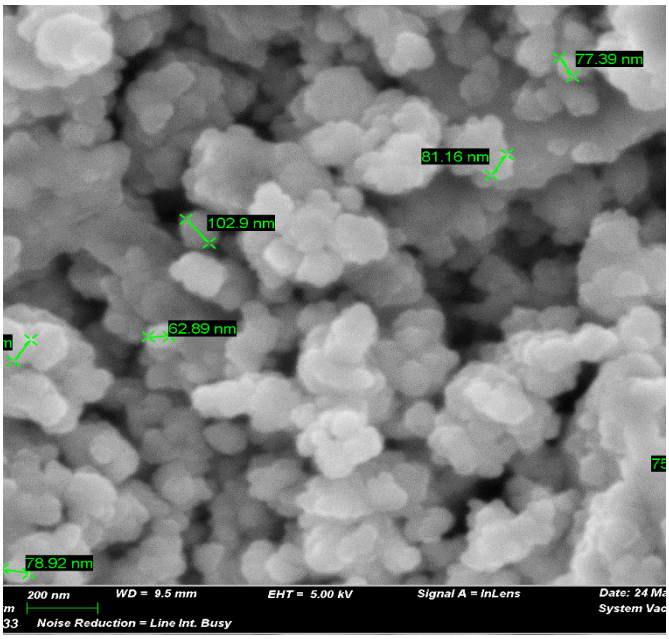

Figure 2. SEM image of $GeBi_2Te_4$ nanopowder after high-energy ball milling (HEBM).

3.2. Dielectric Properties of PVA and $GeBi_2Te_4$/PVA Composites

Dielectric measurements were performed using an E7-20 impedance analyzer in the frequency range from 120 Hz to 10^6 Hz and at temperatures between 20 and 100 °C.

Based on the measured experimental data, the frequency spectra of the real (ε′) and imaginary (ε″) parts of the dielectric permittivity, as well as the frequency dependence of the electrical conductivity (σ), were obtained.

Figure 3(a–d) and Figure 4(a–d) show the frequency dependences of the dielectric permittivity (ε′), dielectric loss function (ε″), dielectric loss tangent (tan δ), and electrical conductivity (σ) measured at temperatures of 20, 40, 60, 80, and 100 °C for pure PVA (Figure 3) and the $GeBi_2Te_4$/PVA composite (Figure 4), respectively.

As the frequency decreases from 10^6 Hz to 100 Hz, the value of ε′ for pure PVA gradually increases from 3.15 (at 10^6 Hz) to 3.38 (at 100 Hz) at room temperature (Figure 3a). With increasing temperature, the dielectric permittivity increases significantly. At a frequency of 10^6 Hz, ε′ increases from 3.15 at room temperature to 6.44 at 100 °C, whereas at 100 Hz the temperature-induced increase is even more pronounced, from 3 at 20 °C to 48.76 at 100 °C.

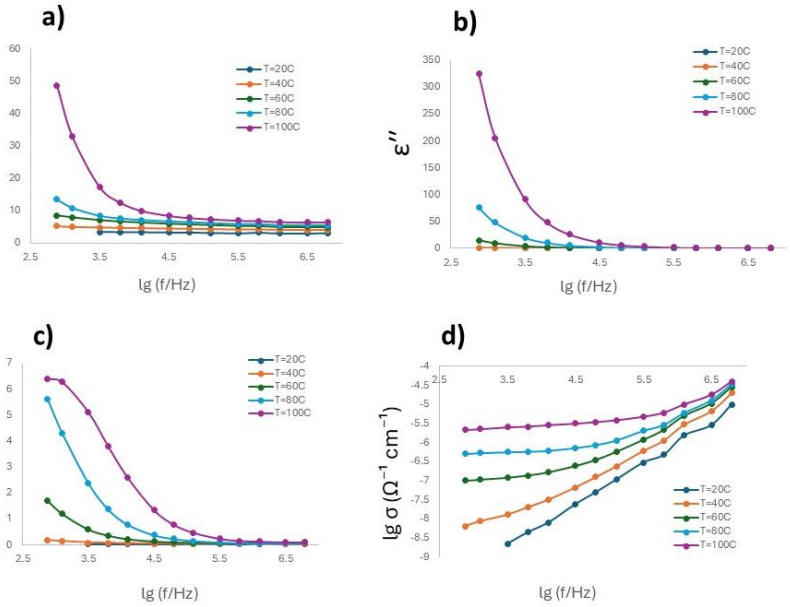

Figure 3. Frequency dependences of (a) dielectric permittivity (ε'), (b) dielectric loss function (ε''), (c) dielectric loss tangent (tan δ), and (d) electrical conductivity (σ) of pure PVA measured at temperatures of 20, 40, 60, 80, and 100 °C.

The dielectric loss function ε'' of pure PVA also increases with decreasing frequency and increasing temperature (Figure 3b). The temperature-induced increase is particularly significant at low frequencies. For example, at a frequency of 120 Hz, ε'' increases from 0.08 at 20°C to 325 at 100°C. The dielectric loss tangent (Figure 3c) exhibits a similar frequency–temperature dependence. The electrical conductivity of pure PVA (Figure 3d) also increases with increasing frequency and temperature.

Such frequency–temperature behavior of the dielectric functions is characteristic of pure PVA polymers [21]. The dielectric permittivity and dielectric losses in the frequency range 10^2–10^6 Hz are governed by dipolar and interfacial polarization processes and by the conductivity of free charge carriers within the PVA matrix. It should be noted that hydroxyl (–OH) groups play a significant role in these processes. In addition, residual moisture in PVA samples strongly affects the magnitude of the dielectric functions.

Figure 4 presents the frequency dependences of the dielectric functions of composite samples consisting of semiconducting $GeBi_2Te_4$ inclusions dispersed in the

PVA matrix. In general, the frequency and temperature dependences of the dielectric functions in this composite are similar to those observed for the PVA matrix. However, the maximum values obtained at a frequency of 100 Hz and a temperature of 100 °C in the composite are significantly lower, reaching 12.49 for ε' (Figure 4a) and 6.57 for ε'' (Figure 4b).

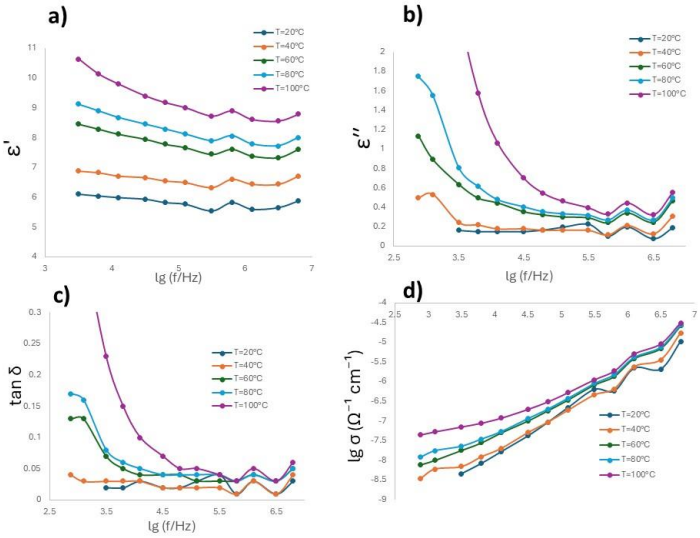

Figure 4. Frequency dependences of (a) dielectric permittivity (ε'), (b) dielectric loss function (ε''), (c) dielectric loss tangent (tan δ), and (d) electrical conductivity (σ) of the $GeBi_2Te_4$/PVA composite measured at temperatures of 20, 40, 60, 80, and 100 °C.

However, in the frequency range $10^{5.5}$–$10^{6.5}$ Hz, characteristic features in the form of maxima are observed in the spectra (Figures 4b and 4c). As the temperature increases, these maxima shift toward lower frequencies. This feature, namely the appearance of peaks in the dielectric spectra, may be associated with polarization occurring at the interface between the electrically conductive semiconductor and the dielectric polymer matrix.

The electrical conductivity of the composite (Figure 4d) increases with increasing frequency and temperature. For example, at a frequency of 500 Hz, the conductivity increases from 4.54×10^{-9} Ω^{-1} cm^{-1} at 40 °C to 7.6×10^{-8} Ω^{-1} cm^{-1} at 100 °C.

The electrical conductivity of the composites is close to that observed for the PVA matrix. This indicates that despite the relatively high volume fraction of $GeBi_2Te_4$ inclusions in the composite (16 vol.%), having an electrical conductivity σ_2 = 128 Ω^{-1} cm^{-1}, no percolation occurs at this semiconductor concentration, and the conductivity is mainly determined by the polymer matrix.

The dielectric response and dielectric losses of the composites can be considered

within the framework of effective medium theory. In composite materials containing electrically conductive filler inclusions, the dielectric permittivity and dielectric loss function are commonly described using the Maxwell–Wagner–Sillars (MWS) model of macroscopic polarization [22,23].

For the case of spherical inclusions, the MWS equations are expressed as follows:

$$\varepsilon' = \varepsilon'_{\infty}\left(1 + \frac{k}{1+\omega^2\tau^2}\right), \tag{1}$$

$$\varepsilon'' = \frac{\varepsilon'_{\infty} k\omega\tau}{1+\omega^2\tau^2}, \tag{2}$$

$$\varepsilon'_{\infty} = \varepsilon'_1\left(1 + \frac{3f(\varepsilon'_2 - \varepsilon'_1)}{2\varepsilon'_1 + \varepsilon'_2}\right), \tag{3}$$

$$K = \frac{9f(\varepsilon'_2 - \varepsilon'_1)}{2\varepsilon'_1 + \varepsilon'_2}, \tag{4}$$

$$\tau = \frac{\varepsilon'_{\infty}(2\varepsilon'_1 - \varepsilon'_2)}{\sigma_1 + \sigma_2} = \varepsilon'_{\infty}(2\varepsilon'_1 + \varepsilon'_2)\rho^2, \tag{5}$$

where ε'_1 and ε'_2 are the real parts of the dielectric permittivity of the matrix and inclusions, respectively; σ_1 and σ_2 are the electrical conductivities of the matrix and inclusions, respectively; ρ is the electrical resistivity; f is the volume fraction of inclusions in the composite; ε'_{∞} is the high-frequency dielectric permittivity; τ is the relaxation time; and ω is the angular frequency.

As follows from the above equations, ε′ and ε″ of the matrix and inclusions depend on the relaxation time τ. The relaxation time corresponding to the maximum is equal to the reciprocal of the peak frequency, $\tau = 1/\omega_{max}$. Since in our composites $\sigma_1 \ll \sigma_2$, σ_1 can be neglected in comparison with σ_2 in Eq. (5). Therefore, the relaxation time is also inversely proportional to the electrical conductivity of the inclusions. Consequently, the shift of the peak toward lower frequencies (and, correspondingly, the increase in relaxation time τ) with increasing temperature in the dielectric spectra indicates a negative temperature dependence of the electrical conductivity of $GeBi_2Te_4$ crystals, i.e., a decrease in conductivity with increasing temperature.

4. Conclusions

$GeBi_2Te_4$/PVA nanocomposites were successfully prepared using $GeBi_2Te_4$ nanopowders obtained by high-energy ball milling (HEBM). Dielectric spectroscopy measurements revealed a pronounced dependence of the dielectric properties on

frequency and temperature. The composite exhibited dielectric behavior similar to that of the PVA matrix; however, relaxation features observed in the high-frequency region were attributed to Maxwell–Wagner–Sillars interfacial polarization at the $GeBi_2Te_4$/PVA interfaces. The electrical conductivity increased with increasing frequency and temperature and remained close to that of pure PVA, indicating the absence of a percolation network at the investigated filler concentration. The observed shift of the relaxation maxima toward lower frequencies with increasing temperature suggests a negative temperature coefficient of conductivity for $GeBi_2Te_4$ inclusions. These results demonstrate that $GeBi_2Te_4$ is a promising filler for tuning the dielectric properties of PVA-based composites.

References

[1] Novoselov K.S.; Mishchenko A.; Carvalho A.; Castro Neto A.H. 2D materials and van der Waals heterostructures. *Science*. 2016, **353**, p. aac9439.

[2] Geim A.K.; Grigorieva I.V. Van der Waals heterostructures. *Nature*. 2013, **499**, p. 419–425.

[3] Duong D.L.; Yun S.J.; Lee Y.H. Van der Waals layered materials: opportunities and challenges. *ACS Nano*. 2017, **11**, p. 11803–11830.

[4] Chhowalla M.; Shin H.S.; Eda G.; Li L.J.; Loh K.P.; Zhang H. The chemistry of two-dimensional layered transition metal dichalcogenide nanosheets. *Nature Chemistry*. 2013, **5**, p. 263–275.

[5] Giri A. et al. Layer-structured anisotropic metal chalcogenides. *Chemical Reviews*. 2023, **123**, p. 2526–2608.

[6] Coleman J.N. et al. Two-dimensional nanosheets produced by liquid exfoliation of layered materials. *Science*. 2011, **331**, p. 568–571.

[7] Kim H.; Abdala A.A.; Macosko C.W. Graphene/polymer nanocomposites. *Macromolecules*. 2010, **43**, p. 6515–6530.

[8] Stankovich S. et al. Graphene-based composite materials. *Nature*. 2006, **442**, p. 282–286.

[9] Dang Z.M. et al. Fundamentals, processes and applications of high-permittivity polymer-matrix composites. *Progress in Materials Science*. 2012, **57**, p. 660–723.

[10] Ramajo L.; Reboredo M.; Castro M. Dielectric response and relaxation phenomena in composites of epoxy resin with $BaTiO_3$ particles. *Composites Part A: Applied Science and Manufacturing*. 2005, **36**, p. 1267–1274.

[11] Sillars R.W. The properties of a dielectric containing semiconducting particles of various shapes. *Journal of the Institution of Electrical Engineers*. 1937, **80**, p. 378–394.

[12] Marcinkova A. et al. Topological metal behavior in $GeBi_2Te_4$ single crystals. *Physical Review B*. 2013, **88**, p. 165128.

[13] Dong J.; Hu L.; Liu J.; Liu Y.; Jiang Y.; Yu Z.; Tan X.Y.; Suwardi A.; Zheng Q.; Li Q.; Li J.F.; Dravid V.P.; Yan Q.; Kanatzidis M.G. Off-centering of Ge atoms in $GeBi_2Te_4$ and impact

on thermoelectric performance. *Advanced Functional Materials*. 2024, **34**, p. 2314499.

[14] Cava R.J.; Ji H.; Fuccillo M.K.; Gibson Q.D.; Hor Y.S. Crystal structure and chemistry of topological insulators. *Journal of Materials Chemistry C*. 2013, **1**, p. 3176–3189.

[15] Addayeva Z.; Muradov M.; Niftiyev N.; Mammedov F.; Eyvazova G.; Filiz B.C. Dielectric spectroscopy of PVA/GO/$FeGaInS_4$ hybrid films: thermal and compositional effects. *Journal of Materials Science*. 2025.

[16] Abdullah A.M.; Aziz S.B.; Saeed S.R. Structural and electrical properties of poly(vinyl alcohol) (PVA): methyl cellulose (MC) based solid polymer blend electrolytes inserted with sodium iodide (NaI) salt. *Arabian Journal of Chemistry*. 2021, **14**, p. 103388.

[17] Gojayev E.M.; Ismailova A.Y.; Mammadova S.I.; Djafarova G.S. Temperature-frequency characteristics of dielectric properties of compositions LDPE + xvol%Bi_2Te_3. *Open Journal of Organic Polymer Materials*. 2016, **6**, p. 25–29.

[18] Kremer F.; Schönhals A. (eds.). *Broadband Dielectric Spectroscopy*. Springer, Berlin, 2003.

[19] Fecht H.J.; Hellstern E.; Fu Z.; Johnson W.L. Nanocrystalline metals prepared by high-energy ball milling. *Metallurgical Transactions A*. 1990, **21**, p. 2333–2337.

[20] Gateshki M.; Petkov V.; Williams G.; Pradhan S.K.; Ren Y. Atomic-scale structure of nanocrystalline ZrO_2 prepared by high-energy ball milling. *Physical Review B*. 2005, **71**, p. 224107.

[21] Nikitina E.A.; Kapralova V.M.; Sudar N.T.; Studzinsky V.M.; Gerasimov V.I. Electrical and optical properties of a nanocomposite material based on polyvinyl alcohol and fullerenol. *St. Petersburg Polytechnic University Journal: Physics and Mathematics*. 2024, **17**(3), p. 76–86.

[22] Samet M.; Kallel A.; Serghei A. Maxwell-Wagner-Sillars interfacial polarization in dielectric spectra of composite materials: scaling laws and applications. *Journal of Composite Materials*. 2022, **56**(20), p. 3197–3217.

[23] Xia X.; Zhong Z.; Weng G.J. Maxwell–Wagner–Sillars mechanism in the frequency dependence of electrical conductivity and dielectric permittivity of graphene-polymer nanocomposites. *Mechanics of Materials*. 2017, **109**, p. 42–50.